THE JOURNAL OF BIOLOGICAL CHEMISTRY VOL. 291, NO. 50, pp. 25999–26012, December 9, 2016

Lysyl Oxidase-like-2 Cross-links Collagen IV of Glomerular Basement Membrane*

Received for publication, May 17, 2016, and in revised form, October 6, 2016 Published, JBC Papers in Press, October 21, 2016, DOI 10.1074/jbc.M116.738856

Carolina Añazco[‡§1,2], Alberto J. López-Jiménez[‡§1], Mohamed Rafi[‡], Lorenzo Vega-Montoto[‡§3], Ming-Zhi Zhang[‡], Billy G. Hudson[‡§], and Roberto M. Vanacore[‡§4]

From the [‡]Division of Nephrology and Hypertension, Department of Medicine, and [§]Center for Matrix Biology, Vanderbilt University Medical Center, Nashville, Tennessee 37232

Edited by Amanda Fosang

The 7S dodecamer is recognized as an important structural cross-linking domain of collagen IV networks that provide mechanical stability to basement membranes, a specialized form of extracellular matrix essential for the development and maintenance of tissue architecture. Although the 7S dodecamer is stabilized by covalent cross-linking, the molecular mechanism by which such cross-links are formed has not been revealed. Here, we aimed to identify the enzyme(s) that cross-links the 7S dodecamer and characterize its expression in the kidney glomerulus. Pharmacological inhibition of candidate extracellular matrix enzymes revealed that lysyl oxidase activity is required for cross-linking of 7S polypeptides. Among all lysyl oxidase family members, lysyl oxidase-like-2 (LOXL2) was identified as the isoform cross-linking collagen IV in mouse embryonal PFHR-9 cells. Biochemical analyses revealed that LOXL2 readily promoted the formation of lysyl-derived cross-links in the 7S dodecamer but not in the NC1 domain. We also established that LOXL2 is the main lysyl oxidase family member present in the glomerular extracellular matrix. Altogether, we demonstrate that LOXL2 is a novel component of the molecular machinery that forms cross-linked collagen IV networks, which are essential for glomerular basement membrane stability and molecular ultrafiltration function.

Collagen IV, the most abundant structural constituent of glomerular basement membrane (GBM),[5] provides a scaffold for the macromolecular assembly of other proteins, confers mechanical strength, and influences cell behavior, features that are indispensable for the normal functioning of the glomerular filtration barrier (1, 2). After secretion into the extracellular space, collagen IV triple helical molecules (protomers) self-assemble into networks by specific end-to-end interactions forming two essential connecting sites: the C-terminal NC1 hexamer and the N-terminal 7S dodecamer (3–6). The NC1 hexamer results from the interaction of two trimeric NC1 domains brought together by extracellular chloride (7, 8). The trimer-trimer interface is enzymatically cross-linked by peroxidasin-catalyzed sulfilimine bonds, an evolutionarily conserved structural feature of collagen IV networks that is essential for tissue development and function (9–14). The 7S dodecamer is also a critical connecting domain for collagen IV network assembly and function (5, 15–17). However, knowledge of the structural and molecular events implicated in assembly and further stabilization of the 7S dodecamer has not been well defined.

The 7S dodecamer is formed by self-assembly of the N-terminal 7S domain of four triple helical protomers. The assembly of all 12 α-chains is stabilized by disulfide and non-disulfide cross-links (15, 18–20). The amino acid sequence of 7S domain contains cysteine and lysine residues, which have been suggested as potential cross-linking sites (21–23). Lysyl residues may be oxidized by lysyl oxidases (LOXs), a family of extracellular enzymes that catalyze the oxidative deamination of the ϵ-amino group of lysine and hydroxylysine residues, promoting the formation of lysyl-derived cross-links (24, 25). The LOX family is composed of five distinct members (LOX, LOXL1, LOXL2, LOXL3, and LOXL4) that share a conserved catalytic domain containing a copper binding site and a quinone cofactor (26, 27). Although proteins of the extracellular matrix (ECM) such as fibril-forming collagens and elastin are cross-linked through a LOX-mediated mechanism (28), it is not clear whether network-forming collagen IV is a substrate for these enzymes. However, a recent phylogenetic study of metazoan genomes to reconstruct the evolutionary history of LOX enzymes suggested that LOXL2, LOXL3, and LOXL4 form a separate superfamily that may be involved in cross-linking basement membrane collagen IV (29).

LOX enzymes regulate many biological processes including extracellular matrix stabilization, cellular growth, and homeostasis (30). The study of lysyl oxidases has gained relevance as

* This work was supported in part by the NIDDK, National Institutes of Health Grants R01 DK099467, R01 DK18381, and R01 DK051265 and Vanderbilt Division of Nephrology faculty development funds. The authors declare that they have no conflicts of interest with the contents of this article. The content is solely the responsibility of the authors and does not necessarily represent the official views of the National Institutes of Health.

[1] Both authors contributed equally to this work.

[2] Supported in part by "Becas-Chile" scholarship provided by the Chilean Government. Present address: Universidad Católica del Maule, Talca 3480112, Chile.

[3] Present address: Idaho National Laboratory, Idaho Falls, ID 83415.

[4] To whom correspondence should be addressed: Dept. of Medicine, Division of Nephrology and Hypertension, Vanderbilt University Medical Center, 1161 21st Ave. S., B-3113 Medical Center N., Nashville, TN 37232. Tel.: 615-322-8323; Fax: 615-343-7156; E-mail: roberto.vanacore@vanderbilt.edu.

[5] The abbreviations used are: GBM, glomerular basement membrane; LOX, lysyl oxidase; LOXL, lysyl oxidase-like; BAPN, β-aminopropionitrile; BCS, bathocuproine disulfonic acid; SCZ, semicarbazide; DNPH, 2,4-dinitrophenylhydrazine; MudPIT, multidimensional protein identification technology; HBSS, Hank's balanced salt solution; qPCR, quantitative PCR; GECM, glomerular ECM.

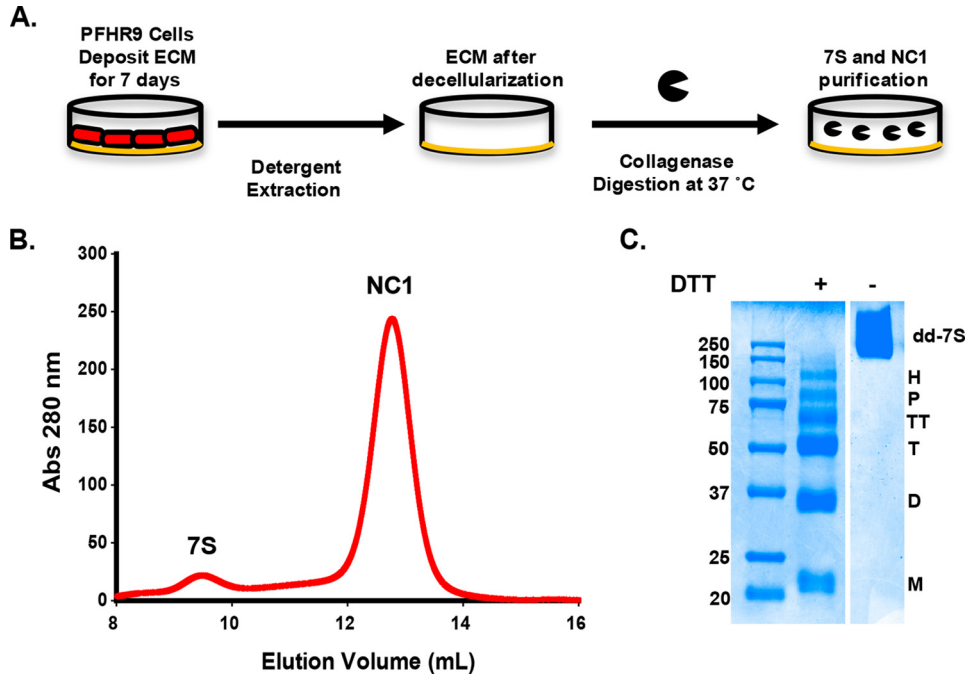

FIGURE 1. **Purification of 7S dodecamers from PFHR-9 cells.** *A* shows a schematic representation of the procedures to purify the 7S dodecamer and NC1 hexamer from PFHR-9 cell matrix. PFHR-9 cells are cultured for 7 days after they reach confluence, allowing the deposition of a very thick ECM. Cells are removed with deoxycholate detergent, and the insoluble ECM is digested with bacterial collagenase. The collagenase-resistant 7S dodecamer and NC1 hexamer are readily solubilized and further purified by ion exchange and gel filtration chromatography. *B*, a representative gel filtration chromatography profile from which 7S dodecamer and NC1 hexamer are purified. *C*, SDS-PAGE analysis of purified 7S dodecamer. Molecular mass standard proteins are shown in kDa. Under non-reducing conditions (− DTT), the 7S dodecamer (*dd-7S*) appears as a single broad band with an apparent molecular weight of ~250,000. This is in agreement with the combined size of 12 monomeric polypeptide chain of ~21,000 each, all of which cross-linked together by disulfide and non-disulfide cross-links. Under reducing conditions (+ DTT), the 7S dodecamer dissociates into six major subunits, monomer (*M*), dimer (*D*), trimer (*T*), tetramer (*TT*), pentamer (*P*), and hexamer (*H*). All subunits, except for monomers, are held together by non-disulfide covalent cross-links. *Abs*, absorbance.

up-regulation of their expression correlates with fibrotic diseases in many different tissues including liver, lung, and kidney (31–33). In addition, members of the family, in particular LOX and LOXL2, have been widely associated with cancer progression and metastasis (31, 34–36). In most cases, these enzymes are thought to cross-link elastin and interstitial collagens. However, LOXL2 appears to be unique in that it has been the only LOX family member involved in regulating the deposition of collagen IV networks in endothelial basement membranes of blood vessel (37).

In this study, we aimed to identify enzymes that cross-link the 7S domain and to characterize their expression in the kidney glomerulus where the stability of collagen IV networks plays a critical role for kidney function. Biochemical, mass spectrometry, and cell culture studies revealed that LOXL2 cross-links the 7S domain of collagen IV. Our findings demonstrate that LOXL2 is the predominant lysyl oxidase family member in the glomerular ECM, a feature that may be important for stabilization of basement membranes.

Results

Characterization of the 7S Dodecamer of PFHR-9 Collagen IV—Collagen IV is the most abundant structural component of basement membranes where it plays an important functional role in development and in structural stability and architecture of tissues (38). Although the occurrence of covalent cross-links stabilizing the assembly of 7S domains of collagen IV molecules has been suggested previously (20, 23), to date there is no knowledge of which enzyme(s) is involved in this process. Therefore, we aimed to identify the enzyme(s) responsible for cross-linking of 7S domain using PFHR-9 cells, which were shown previously to produce collagen IV networks and peroxidasin, the enzyme that catalyzes the formation of sulfilimine cross-links in the C-terminal NC1 domains (11).

PFHR-9 cells were cultured for extended periods of time after reaching confluence to allow for collagen IV network deposition (Fig. 1*A*). Similar to what is observed in animal tissues, collagenase digestion of PFHR-9 matrix yields the two predominant cross-linking domains of collagen IV networks: the NC1 hexamer and 7S dodecamer (Fig. 1*B*). In SDS-PAGE under non-reducing conditions, the purified 7S dodecamer is observed with an apparent molecular weight of ~250,000 (Fig. 1*C*), which is in agreement with the combined size of 12 polypeptide chains of ~21,000 each. Reductive cleavage of disulfide bonds revealed that 12 polypeptide chains within the 7S dodecamer are organized into monomers and five oligomeric subunits (Fig. 1*C*, *right lane*) including dimers, trimers, tetramers, pentamers, and hexamers. The presence of these oligomeric subunits after strong denaturing conditions of SDS-PAGE clearly indicates that the 7S dodecamer is cross-linked by non-disulfide covalent cross-links.

Lysyl Oxidase Inhibitors Block the Formation of Non-disulfide Cross-links in the 7S Dodecamer—To elucidate the type of bonds that cross-link the 7S subunits, PFHR-9 cells were cultured in the presence of several pharmacological inhibitors of

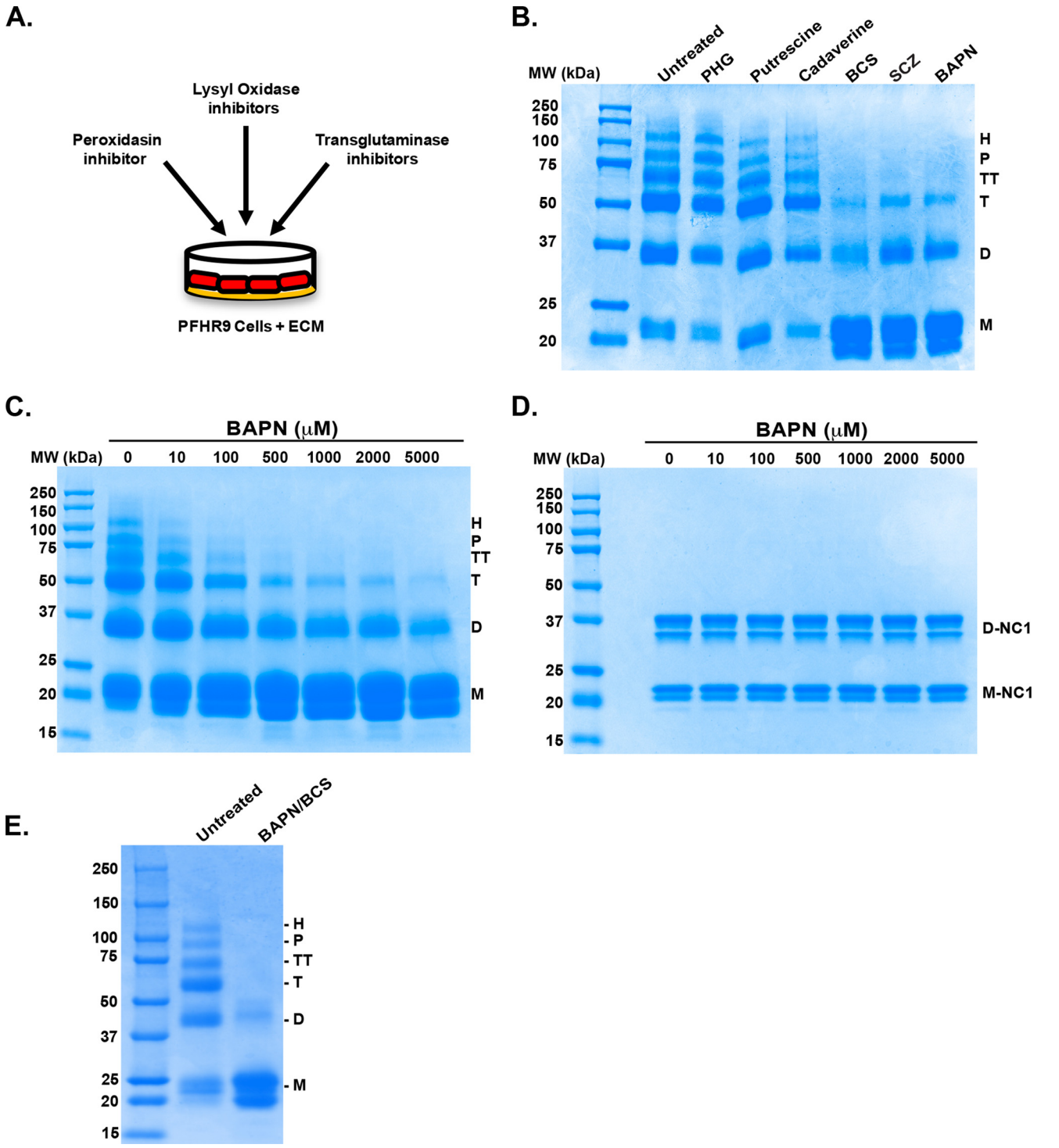

FIGURE 2. **7S subunits are stabilized by LOX-mediated cross-links.** *A*, schematic representation of the experimental strategy to evaluate the effect of enzyme inhibitors and copper chelators on cross-linking of 7S dodecamer. *B*, PFHR-9 cells were grown in the presence of the indicated enzyme inhibitors for 7 days. 7S dodecamers were purified and analyzed by SDS-PAGE under reducing conditions. The inhibitors and concentrations used were as follows: 5 mM cadaverine and 5 mM putrescine (transglutaminase inhibitors), 1 mM BAPN (lysyl oxidase inhibitor), 50 μM phloroglucinol (*PHG*) (peroxidasin inhibitor), and 100 μM BCS and 1 mM SCZ (copper chelators). *C*, SDS-PAGE analysis under reducing conditions of 7S dodecamers purified from PFHR-9 cells grown for 7 days in the presence of increasing concentrations of BAPN (10–5000 μM). *D*, SDS-PAGE analysis under non-reducing conditions of NC1 hexamers purified from PFHR-9 matrix produced in *C*. *E*, SDS-PAGE analysis under reducing conditions of 7S dodecamers purified from untreated (control) cells and cells grown in culture medium containing 1 mM BAPN and 100 μM BCS. *M*, *D*, *T*, *TT*, *P*, and *H* indicate the electrophoretic mobility of monomer, dimer, trimer, tetramer, pentamer, and hexamer 7S subunits, respectively. *D-NC1* and *M-NC1* indicate the electrophoretic migration of NC1 dimers and NC1 monomers, respectively. The migration of molecular weight (*MW*) standard proteins is shown on the *left*.

matrix-cross-linking enzymes including inhibitors of transglutaminase (cadaverine and putrescine), peroxidasin (phloroglucinol) and lysyl oxidases (β-aminopropionitrile (BAPN), bathocuproine disulfonic acid (BCS), and semicarbazide (SCZ)) (Fig. 2*A*). Cells were allowed to deposit collagen IV into the matrix for 7 days after confluence, replacing culture medium contain-

ing inhibitors every day. Although transglutaminase and peroxidasin inhibitors did not have any effect on 7S cross-linking, the irreversible inhibitor of lysyl oxidase, BAPN, completely prevented the formation of hexameric, pentameric, and tetrameric 7S subunits (Fig. 2*B*). A concomitant increase in monomer subunits was observed with the concurrent decrease of high molecular weight subunits. Because 7S trimeric and dimeric subunits remained after treatment with BAPN, we performed a dose-response experiment in which PFHR-9 cells were cultured with BAPN concentrations up to 5 mM to ensure complete inhibition of lysyl oxidase activity (Fig. 2*C*). Maximal inhibition was achieved between 0.5 and 1 mM concentration of BAPN, which is the normal range used for the inhibition of lysyl oxidase activity in cultured cells (39, 40). Higher concentrations up to 5 mM BAPN had very little effect on the 7S subunits profile, but survival of PFHR-9 cells was significantly decreased especially at the highest 5 mM concentration. Notably, BAPN, even at the higher concentrations, did not have any effect on NC1 domain sulfilimine cross-linking as the dimeric subunits remained unchanged (Fig. 2*D*).

Because all members of the lysyl oxidase family use copper as a cofactor that is essential for enzymatic activity (24), we cultured PFHR-9 cells with specific copper chelators as an alternative mechanism to inhibit lysyl oxidase activity. As shown in Fig. 2*B*, membrane-impermeable copper chelator BCS and SCZ, an inhibitor of semicarbazide-sensitive amine oxidase, inhibited the formation of hexameric, pentameric, and tetrameric 7S subunits, preventing the formation of cross-links in a manner similar to BAPN. Although the conditions used to inhibit lysyl oxidase activity significantly reduced the intensity of 7S subunits of high molecular weight, trimeric and dimeric subunits persisted.

As BAPN and BCS could each partially inhibit LOX activity through different mechanisms, we tested whether culturing PFHR-9 cells in the presence of these two inhibitors would have a synergistic effect on the inhibition of cross-linked 7S subunits. As shown on Fig. 2*E*, SDS-PAGE analyses under reducing conditions revealed that the combined use of BAPN and BCS drastically inhibits the formation of cross-linked 7S subunits. Although a small amount of 7S dimers remained, this form of the 7S dodecamer (7S-BAPN/BCS) is predominantly composed by monomeric subunits, indicating that BAPN and BCS achieved a more efficient inhibition of lysyl oxidase activity than BAPN or BCS alone (Fig. 2*B*). In summary, these data demonstrate that lysyl oxidase enzymatic activity catalyzes the formation of non-disulfide covalent cross-links stabilizing 7S dodecamers.

LOXL2 Is the Most Abundant Lysyl Oxidase Isoform in PFHR-9 Matrix—Because LOX family is composed of five members, we characterized the relative expression of all LOX family members in PFHR-9 cells to identify the specific LOX enzyme cross-linking the 7S dodecamer. We isolated mRNA from PFHR-9 cells to perform quantitative RT-PCR. As observed in Fig. 3*A*, LOXL2 is the predominant isoform detected in PFHR-9 cells with a relative abundance of more than a 1000 times the expression level of the other LOX family members. Shotgun proteomics analysis was also performed to identify which of the five members of the LOX family was present in the PFHR-9 matrix (Fig. 3*C*). The deoxycholate-insoluble ECM proteins were extracted with 2 M guanidine HCl, and the soluble proteins were digested with trypsin and analyzed by LC-MS/MS. The results indicated that LOXL2 was the only lysyl oxidase family member identified in PFHR-9 matrix. Sixteen unique peptides were detected, representing about 45% of the LOXL2 sequence. To confirm the presence of LOXL2 in the extracellular matrix of PFHR-9 cells, immunoblotting analyses were performed. Fig. 3*B* shows that LOXL2 occurs as a 100-kDa polypeptide and as a smaller 67-kDa polypeptide. These two forms of LOXL2 have been observed in other cell types and tissues with the smaller 67-kDa form resulting from proteolytic N-terminal processing by an unknown protease (34, 41). These data demonstrate that LOXL2 is the predominant isoenzyme expressed by PFHR-9 cells and that the enzyme is present in the insoluble matrix.

LOXL2 Promotes Cross-linking of the 7S Dodecamer of Collagen IV—To elucidate whether LOXL2 is responsible for catalyzing the formation of lysyl-derived cross-links in the 7S domain, we performed *in vitro* cross-linking assays (Fig. 4). Thus, 7S-BAPN/BCS was incubated with recombinant human LOXL2, and the products of the reaction were analyzed by SDS-PAGE. As shown in Fig. 4, LOXL2 led to a significant increased formation of high molecular weight 7S subunits (dimer, trimer, tetramer, pentamer, and hexamer) at the expense of the monomeric subunits. This result indicates that the LOXL2 cross-links the 7S dodecamer of collagen IV *in vitro*.

To test whether LOXL2 can promote the formation of cross-links in the 7S dodecamer within the native insoluble collagen IV network, HEK293 cells were overlaid onto BAPN-treated PFHR-9 matrix and transiently transfected with plasmids containing either human LOXL2 or a catalytically inactive LOXL2^{Y689F} mutant (Fig. 5*A*). LOXL2^{Y689F} is a catalytically inactive mutant in which Tyr-689 was mutated to phenylalanine, preventing the formation of lysyl tyrosyl quinone cofactor that is required for oxidase activity (27, 42). Seventy-two hours after transfection, LOX enzymatic activity was clearly evident in the medium of cells transfected with LOXL2 cDNA but absent in LOXL2^{Y689F} mutant (Fig. 5*B*). The expression of recombinant proteins was verified by immunoblotting with anti-LOXL2 (Fig. 5*B*, *inset*). HEK293 cells were removed by detergent extraction, and the remaining insoluble matrix proteins were digested with collagenase. Solubilized proteins were analyzed by SDS-PAGE to visualize the integrity of 7S dodecamer and NC1 monomeric and dimeric subunits (Fig. 5*C*). Immunoblotting analyses of 7S dodecamers isolated from PFHR-9 matrix exposed to active recombinant LOXL2 showed that 7S cross-linking had occurred, reestablishing the high molecular weight subunits including hexamer, pentamer, and tetramer 7S subunits (Fig. 5*D*). Overexpression of the LOXL2^{Y689F} mutant had no effect on the 7S subunit profile and closely resembles the profile shown by the control cells transfected with empty vector (mock). Notably, NC1 monomeric and dimeric subunits remained unchanged in all conditions (Fig. 5*C*), indicating that LOXL2-mediated cross-linking is restricted to the 7S dodecamer. In summary, these studies demonstrate that the catalytic activity of LOXL2 is required to pro-

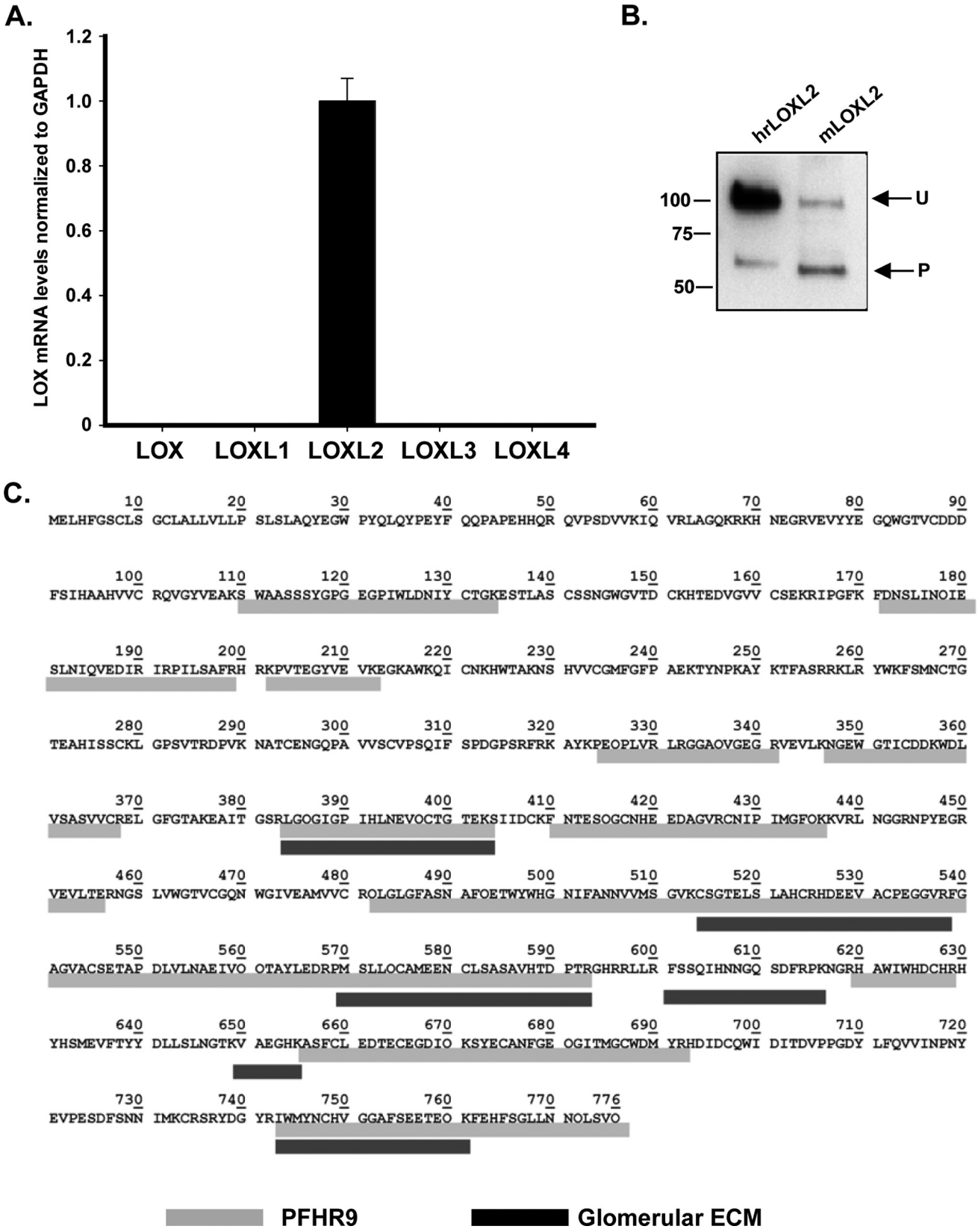

FIGURE 3. **LOXL2 is the main lysyl oxidase expressed in PFHR-9 matrix.** *A*, the qPCR studies show the detection of LOXL2 as the only LOX isoform expressed in PFHR-9 cells. *Error bars* represent S.D. from three independent experiments. *B*, Western blotting detection of LOXL2 protein in a 4 M urea extract from PFHR-9 matrix. Detection of unprocessed (*U*) and processed (*P*) forms of LOXL2 from PFHR-9 matrix is similar to the profile observed for human recombinant LOXL2 (*hrLOXL2*) that was used as a control. *C*, mass spectrometry identification of mouse LOXL2 (*mLOXL2*) peptides extracted from PFHR-9 matrix (*gray*) and glomerular ECM (*black*).

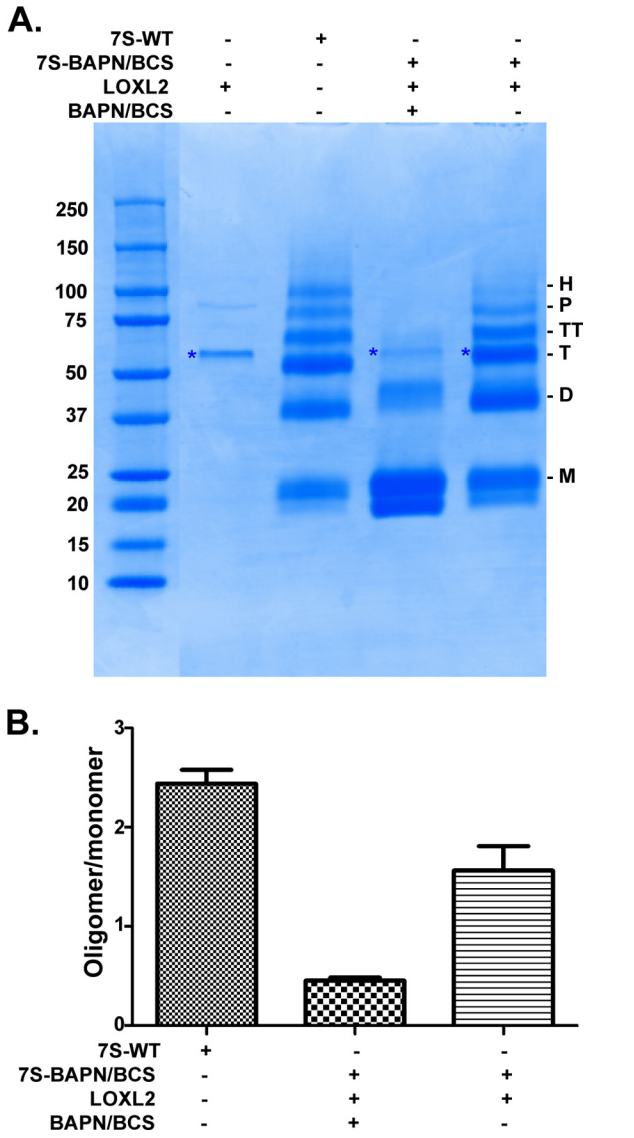

FIGURE 4. ***In vitro* cross-linking of 7S dodecamer with LOXL2.** *A*, SDS-PAGE analysis under reducing conditions of *in vitro* cross-linking reaction of 7S-BAPN/BCS by LOXL2-His_6. The *asterisk* denotes the electrophoretic migration of recombinant LOXL2-His_6. *M*, *D*, *T*, *TT*, *P*, and *H* indicate the electrophoretic mobility of monomer, dimer, trimer, tetramer, pentamer, and hexamer 7S subunits, respectively. *B*, quantitation of signal intensities of cross-linked 7S subunits (dimer, trimer, tetramer, pentamer, and hexamer) relative to 7S monomers (uncross-linked) for each lane from three independent experiments. *Error bars* represent S.E. Molecular mass standards are indicated in kDa on the *left* of each gel.

mote cross-linking of 7S dodecamer, but not the NC1 domain, in the insoluble extracellular matrix.

LOXL2 Forms Aldehyde-derived Cross-links in the 7S Dodecamer—Lysyl oxidases oxidize lysyl and/or hydroxylysyl residues to their aldehyde forms (allysine or hydroxyallysine), which can spontaneously condense into various forms of lysyl-derived cross-links (25, 43). To evaluate whether these free carbonyl groups are being produced during biosynthesis of LOX-mediated cross-linking of the 7S dodecamer in PFHR-9 cell matrix, we used Brady's reagent, 2,4-dinitrophenylhydrazine (DNPH), the classical method for detecting protein carbonyls (44). Immunoblotting performed with anti-DNPH antibody detecting the formation of a hydrazone derivative of DNPH revealed carbonyl groups in dimer, trimer, tetramer, pentamer, and hexamer 7S subunits (Fig. 6). Notably, monomeric 7S subunits were not detected despite being more abundant as evidenced by Coomassie staining. In addition, minimal DNPH reactivity (7S dimers) was observed in 7S-BAPN. However, this protein cross-linked *in vitro* with recombinant human LOXL2 showed a pattern similar to the native 7S dodecamer. As an additional control, we performed the same analysis using purified NC1 hexamers incubated with recombinant LOXL2; however, no DNPH reactivity was observed, suggesting that LOXL2 reactivity is specific for the 7S dodecamer. Taken together, these data indicate that 7S dodecamer is stabilized by carbonyl-containing cross-link structures and that it is a specific substrate for LOXL2.

LOXL2 Is the Predominant Lysyl Oxidase in Mouse Glomerulus—Although members of the lysyl oxidase family are known to be differentially expressed in tissues and cellular types (24, 45), very little information about the expression of these enzymes is available in the kidney glomerulus where collagen IV is abundant. Because we have demonstrated that LOXL2 cross-links the 7S dodecamer and because collagen IV networks play an important role providing structural stability to the glomerular architecture, particularly the GBM, we aimed to determine whether LOXL2 is expressed in the normal kidney glomerulus. For these experiments, we isolated glomeruli by the Dynabead method and extracted mRNA to determine the relative expression profile of the LOX family members by quantitative RT-PCR. Fig. 7*A* shows that LOXL2 is clearly the most abundant transcript followed by a significant amount of LOXL1. Although transcripts for LOX, LOXL3, and LOXL4 were also detected, they were present at much decreased levels. This result suggests that LOXL2 is the predominant lysyl oxidase of the mouse kidney glomerulus.

To confirm that LOXL2 is present in the glomerular ECM, we performed multidimensional protein identification technology (MudPIT) proteomics studies using glomerular ECM proteins extracted from Dynabead-isolated mouse glomeruli. Insoluble glomerular ECM proteins were digested with trypsin to generate peptides that were analyzed using the MudPIT approach described under "Experimental Procedures." Seven peptides derived from LOXL2, representing 14.8% sequence coverage, were found in the mouse glomerular ECM (Fig. 3*C*). Other members of LOX family were not detected in our MudPIT analyses. The presence of LOXL2 in the glomerular ECM was also confirmed by immunoblotting using an anti-LOXL2 antibody (Fig. 7*B*). Similar to PFHR-9 cells, unprocessed and processed forms of LOXL2 were observed in the glomerulus. These correspond to the full-length and proteolytically processed forms of LOXL2 found in other tissues, respectively (41, 46). Thus, the evidence provided by mass spectrometry and immunoblotting clearly demonstrates that LOXL2 is a component of the mouse glomerulus ECM.

We also performed immunohistochemistry studies to determine the distribution and localization of LOXL2 in the mouse glomerulus. Immunostaining of kidney sections with an anti-LOXL2 antibody revealed that although some immunoreactivity is observed in tubular interstitial compartment the signal concentrates in the glomeruli associated with the glomerular

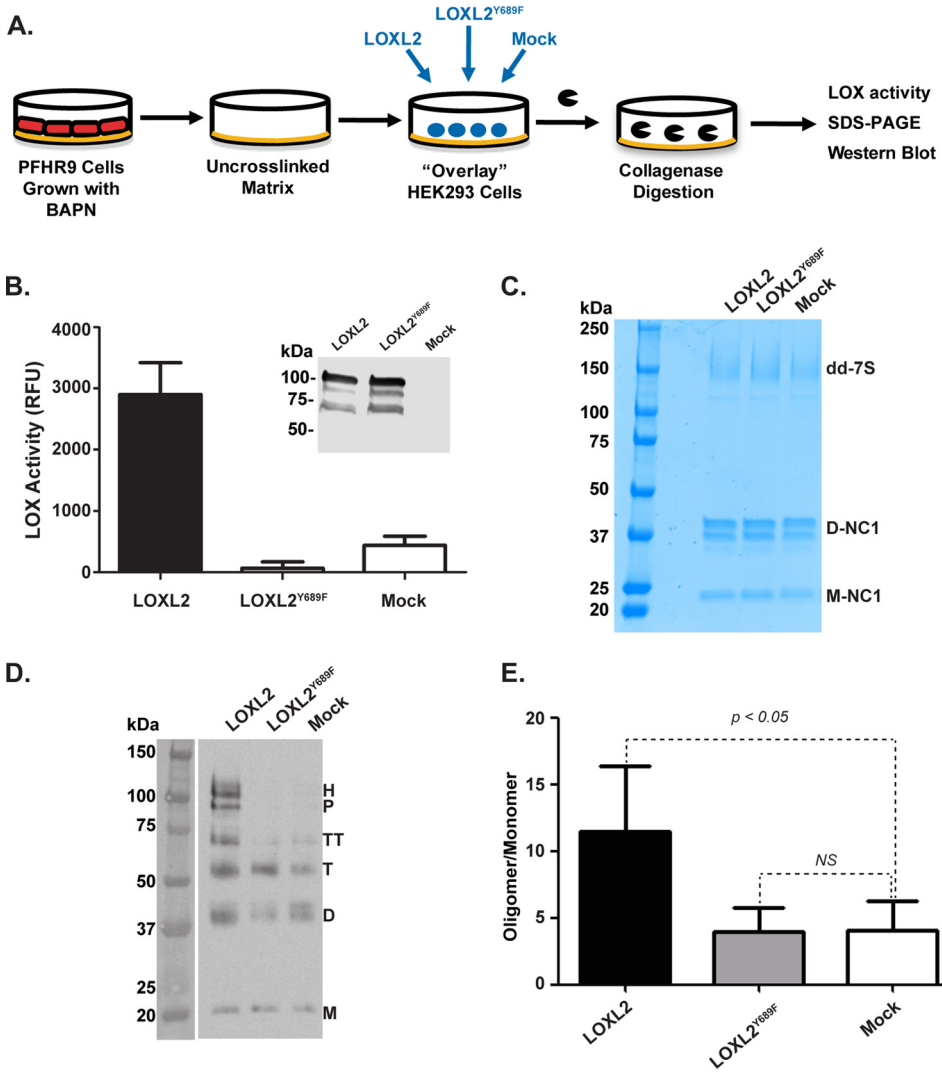

FIGURE 5. **LOXL2 cross-links the 7S dodecamer in a native insoluble basement membrane.** *A*, schematic representation of the overlay assay showing the isolation of PFHR-9 matrix, transient transfection of LOXL2 and LOXL2^{Y689F} of HEK293 cells overlaid on a BAPN-treated substrate matrix, and 7S and NC1 detection after collagenase digestion. *B*, LOX enzymatic activity in the culture medium of HEK293 cells transfected with either LOXL2 or LOXL2^{Y689F} mutant. Expression of enzymes was confirmed by Western blotting analysis using anti-LOXL2 antibody. *Error bars* represent S.D. from three independent experiments. *C*, non-reducing SDS-PAGE analysis of a collagenase digest of PFHR-9 matrices from the overlay assay. *7S-dd*, 7S dodecamer; *D-NC1*, NC1 dimer; *M-NC1*, NC1 monomer. *D*, immunoblotting analysis using anti-7S antibody of protein samples from *C* fractionated under reducing conditions. *M*, *D*, *T*, *TT*, *P*, and *H* indicate the electrophoretic mobility of monomer, dimer, trimer, tetramer, pentamer, and hexamer 7S subunits, respectively. *E*, quantitation of signal intensities of cross-linked 7S subunits (dimer, trimer, tetramer, pentamer, and hexamer) relative to 7S monomers (uncross-linked) for each lane. *Error bars* represent S.D. from three independent experiments. Data were analyzed by *t* test. Statistical significance is shown *above* the *bars*. *NS*, not significant; *RFU*, relative fluorescence units.

capillary loops (Fig. 7). Interestingly, Fig. 7*C* shows that LOXL2 signal is evident in the intracellular compartment of the podocyte and is predominantly perinuclear. A similar immunohistochemistry staining pattern was obtained with a different antibody to LOXL2. Altogether, we have demonstrated that LOXL2 is the main lysyl oxidase expressed in the kidney glomerulus where it can cross-link the 7S dodecamer as an important mechanism to stabilize collagen IV networks in the glomerular ECM.

Discussion

Cross-linking is an important feature of collagen IV networks as they provide structural support to all animal tissues. Two important cross-linking domains are recognized in collagen IV networks, namely the NC1 hexamer and the 7S dodecamer. Although studies of the NC1 hexamer have generated key new discoveries including a novel sulfilimine chemical bond, its catalyzing enzyme peroxidasin, and the recognition of bromide as an essential trace element for animal life (9–12, 47), the last biochemical analyses of the 7S dodecamer trace back to more than 25 years ago (16). Here, we demonstrate that LOXL2 cross-links the 7S domain and thus constitutes another member of the molecular machinery involved in collagen IV biosynthesis.

We performed 7S cross-linking studies in PFHR-9 cells, a well defined cell culture system that recapitulates known structural aspects of collagen IV networks. These cells were used previously to study the assembly of collagen IV triple helical molecules (19) and more recently to identify peroxidasin as the enzyme responsible for the formation of sulfilimine cross-links

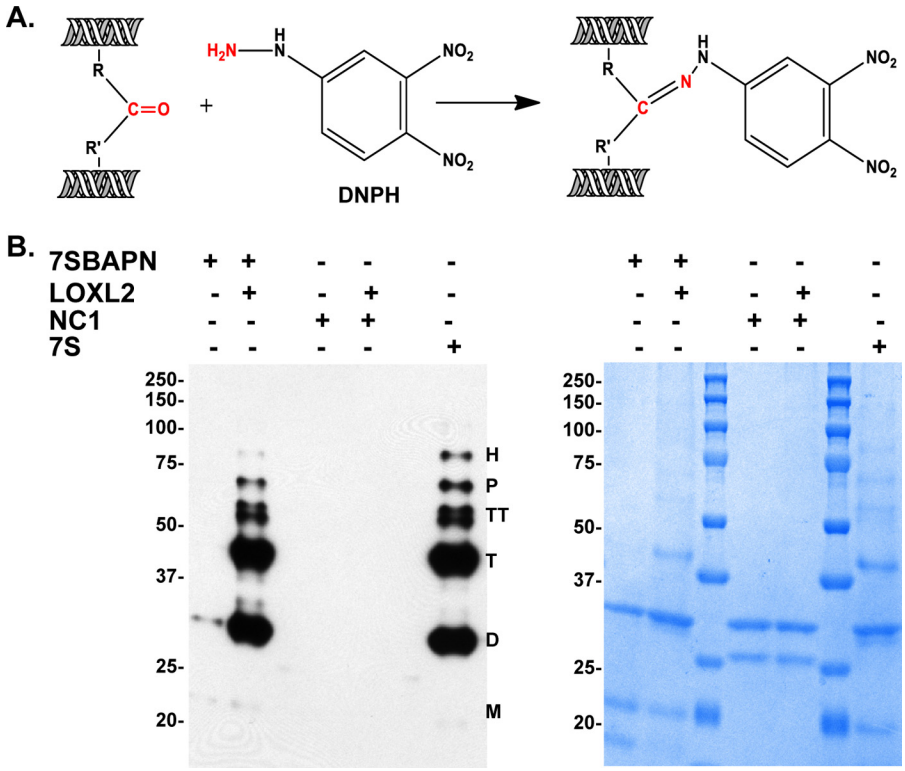

FIGURE 6. **Detection of carbonyl groups in cross-linked 7S subunits.** *A*, schematic representation of the chemical reaction of DNPH with carbonyl groups used for detection of LOX-derived cross-links in 7S subunits. *B*, immunoblotting detection of carbonyl groups in 7S dodecamers isolated from PFHR-9 cells grown with (*7S-BAPN*) and without (*7S*) the lysyl oxidase inhibitor BAPN. 7S-BAPN and NC1 hexamers were incubated overnight at 37 °C with and without purified recombinant LOXL2 to allow for generation of lysyl-derived cross-links. Protein oxidation was detected with the Oxyblot protein oxidation detection kit. *M*, *D*, *T*, *TT*, *P*, and *H* indicate the electrophoretic mobility of monomer, dimer, trimer, tetramer, pentamer, and hexamer 7S subunits, respectively. The panel on the *right-hand side* shows a replica SDS-polyacrylamide gel stained with Coomassie Blue. Molecular mass standard proteins are shown in kDa on the *left* of each gel.

that stabilize the NC1 hexamers (11). The 7S dodecamer results from the self-assembly of the N-terminal sequences of four triple helical collagen IV protomers. The resulting assembly is stabilized by disulfide and non-disulfide cross-links; the formation of the latter is catalyzed by LOXL2 as shown in this study. The soluble 7S dodecamer migrates as an ~250-kDa protein assembly in SDS-PAGE under non-reducing conditions. However, upon reduction of disulfide bonds, the 7S dodecamer dissociates into six distinct subunits: 7S monomers of about 21 kDa corresponding to the N-terminal polypeptide derived from a single α-chain and five higher molecular weight subunits resulting from different oligomerization states of the monomeric subunits forming dimer, trimer, tetramer, pentamer, and hexamer. Although the exact organization of these oligomers within the 7S dodecamer is not clear, they are likely to result from the covalent cross-linking of lysine and/or hydroxylysine residues within as well as between triple helical protomers. Such cross-linking sites have been suggested by alignment of triple helical protomers into three-dimensional models (6, 16, 21, 22), but unambiguous experimental evidence identifying the specific location of lysine/hydroxylysine residues involved in cross-linking is not yet available. Identification of LOXL2 should certainly facilitate future mapping studies aimed at identifying such residues in the 7S dodecamer.

For many years, it has been noted that collagen IV molecules are more soluble in Engelbreth-Holm-Swarm tumors when mice are made lathyritic, which suggested that collagen IV networks are stabilized by LOX-mediated cross-links (23). Further attempts to identify $NaBH_4$-reducible cross-links in collagen IV by classical techniques developed for fibrillar collagens (48) only yielded an unexpected small amount of dihydroxylysinonorleucine, a cross-link resulting from the condensation of hydroxylysine and hydroxyallysine (hydroxylysine aldehyde) residues (20). Because collagen IV preparations used in these classical studies were isolated from placenta tissue, the presence of a small amount of dihydroxylysinonorleucine cross-links was also attributed to possible contamination of the preparation with fibrillar collagens. Furthermore, the absence of other known LOX-derived cross-links such as pyridinolines or pyrroles suggested that in collagen IV cross-links follow a different maturation pathway, forming unknown non-reducible cross-links. Our *in vitro* cross-linking experiments demonstrated that cross-linking of 7S subunits mediated by LOXL2 generates carbonyl groups, which were easily detected by DNPH. Although this evidence does not reveal the exact chemical structure of such cross-links, DNPH is likely to be reacting with newly formed ketoimine groups of hydroxylysine-derived divalent cross-links, a finding that is consistent with analyses of collagen IV from human placenta by Bailey *et al.* (20).

Structural features of 7S dodecamer may control its recognition by LOXL2 and determine specificity for lysine oxidation. Our overlay and DNPH derivatization experiments demonstrated that LOXL2 has a clear preference for the 7S dodecamer as the NC1 domain subunits (monomers and dimers) remained

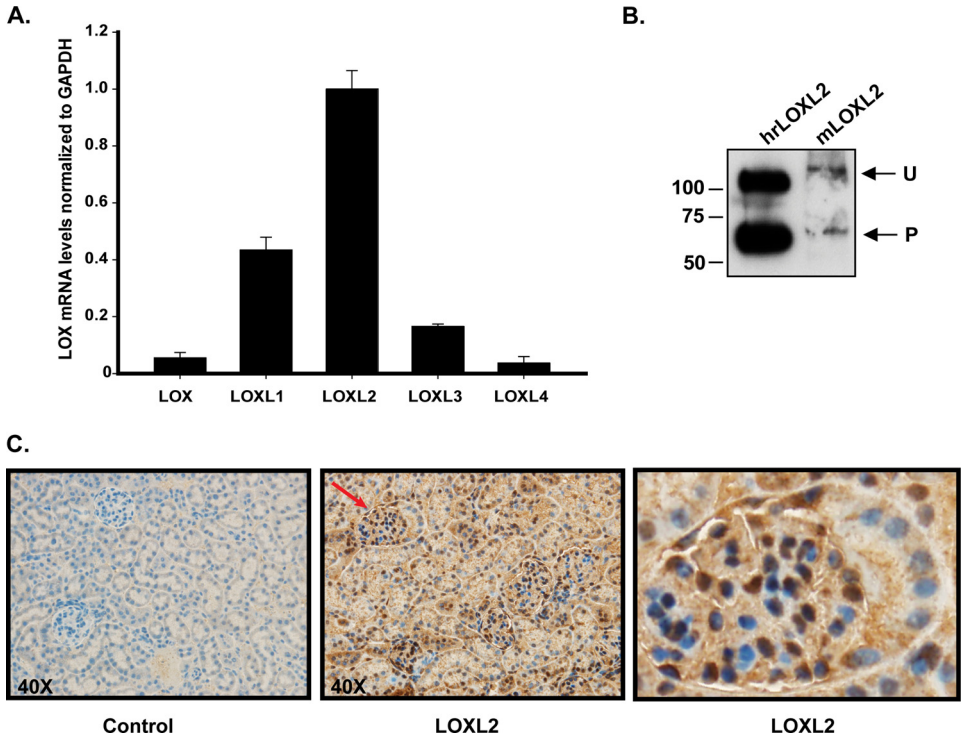

FIGURE 7. **LOXL2 is the predominant lysyl oxidase in the mouse glomerulus.** *A*, RT-PCR analyses of mouse glomerulus showing the relative expression of LOX family members. *Error bars* represent S.D. from three independent experiments. *B*, detection of LOXL2 in the ECM of mouse glomerulus (*mLOXL2*). Human recombinant LOXL2 (*hrLOXL2*) expressed in HEK293 cells is shown for comparison. Unprocessed (*U*) and processed (*P*) forms of LOXL2 are indicated. *C*, immunohistochemical localization of LOXL2 in kidney cortex of adult mouse. The *left* picture shows a control section of the mouse kidney cortex in which the primary anti-LOXL2 antibody was not included. The section was counterstained with Harris's hematoxylin to demonstrate nuclei (*blue*). The *center* picture corresponds to a similar section stained with anti-LOXL2 antibody (*dark brown* precipitate). The picture shown in the *far right* is a magnification of a single glomerulus indicated with the *red arrow* in the *middle* picture.

unchanged. This evidence suggests that LOXL2 targets specific lysine residues within the 7S dodecamer rather than the globular NC1 hexamers. Although obvious structural differences between the two collagenase-resistant domains may account for such preference, it is also possible that LOXL2 may recognize a specific sequence motif such as that found in fibrillar collagens recognized by classical LOX, which modifies the lysine residue found within the tetrapeptide KGHR (20). Interestingly, a similar KGER motif is present within the 7S domain sequence (but absent in the NC1 domain) that may represent potential sites of cross-linking and explain the different cross-linking outcomes of 7S and NC1 subunits. Notably, KGER motifs are also found within the triple helical domain, and thus it is possible that LOXL2 may also oxidize such lysine residues, potentially generating other cross-linking sites between collagen IV molecules.

Interestingly, although addition of BAPN into the culture medium of PFHR-9 cells significantly reduced LOXL2-mediated cross-linking of 7S dodecamer, it did not inhibit the formation of 7S dimeric subunits. BAPN was first shown to be a competitive inhibitor of classical LOX (39, 40), and more recent studies have demonstrated that it inhibits LOXL2 with an IC_{50} of 3.4 μM (49). Our dose-response experiments included concentrations up 5 mM BAPN, which would be expected to fully inhibit LOXL2 enzymatic activity. However, maximal inhibition of 7S subunit formation was only achieved by using both BAPN and the copper chelator BCS, suggesting that these two different mechanisms synergize to achieve maximal inhibition of 7S dodecamer cross-linking (36, 42, 49, 51). Remarkably, despite the absence of lysyl-derived cross-links, 7S-BAPN/BCS dodecamers could still be purified from the insoluble matrix by collagenase digestion, suggesting that 7S dodecamers are formed regardless of lysyl oxidase activity and that disulfides cross-links confer collagenase resistance to the triple helical assembly. These results are consistent with previous studies noting that 7S dodecamer formation is driven by the self-assembly of hydrophobic sequences within the 7S sequences, a process that may occur prior to stabilization by LOXL2-mediated cross-linking (16, 19). Collectively, these results demonstrate that, in addition to disulfide bridges, the association of four triple helical protomers forming the 7S dodecamer is stabilized by LOXL2-mediated cross-linking of lysine and/or hydroxylysine residues.

As the main lysyl oxidase in the kidney glomerulus, LOXL2 through its collagen IV cross-linking function may provide additional mechanical strength to the glomerular extracellular scaffolds including the GBM. LOXL2 and collagen IV have been shown to colocalize in the basement membrane of endothelial cells (37), suggesting a possible involvement of LOXL2 in the stabilization of collagen IV networks during blood vessel formation. Although we anticipated a linear staining around the capillary loops, as is the case for GBM proteins such as collagen IV, LOXL2 perinuclear staining in podocytes suggests that these cells predominantly synthesize the enzyme in mouse glomerulus. However, proteomics and immunoblotting studies of glomerular ECM extracts confirmed that the cross-linking

enzyme, albeit at low levels, is also secreted, suggesting that under normal conditions a minimal extracellular presence of LOXL2 may be sufficient for stabilizing the glomerular ECM. Interestingly, recent gene ablation studies for LOXL2 resulted in perinatal lethality in half of new born mice mainly associated to congenital heart defects (52). The report did not reveal any apparent phenotype indicative of basement membrane malfunction; however, because maintenance and stability of GBM may need the structural reinforcement by additional LOXL2 cross-linking, it will be interesting to investigate whether surviving LOXL2-null animals are more susceptible to renal failure.

In contrast, high throughput studies have reported that LOXL2 up-regulation is observed in renal fibrosis accompanying different types of nephropathies (53–55). LOXL2 has also been associated with ECM remodeling, the development of fibrotic conditions in renal tubulointerstitial fibrosis associated with diabetic and IgA nephropathies, and hypertensive nephrosclerosis (51). It is possible to hypothesize that increased levels of extracellular LOXL2 could lead to excessive cross-linking and contribute to the accumulation of collagen IV in glomerulosclerosis. Collectively, our findings provide an understanding of the mechanisms by which collagen IV molecules are stabilized by LOXL2-mediated covalent cross-linking at the N-terminal 7S domain and provide a framework for future studies aimed at identifying pathogenic mechanisms that interfere with collagen IV homeostasis.

Experimental Procedures

Animal Experiments—The Principles of Laboratory Animal Care were followed according to Institutional Animal Care and Use Committee guidelines. The control group included age-matched wild type C57BLKS mice. Animals were sacrificed at 22 weeks of age.

Cell Culture—HEK293 cells were cultured in Dulbecco's modified Eagle's medium (DMEM) and F-12 Ham's medium (1:1) with 1% penicillamine-streptomycin and incubated at 37 °C in 5% CO_2. PFHR-9 cells were cultured in DMEM supplemented with 10% fetal bovine serum and 1% penicillamine-streptomycin and incubated at 37 °C in 10% CO_2. For 7S dodecamer purification, PFHR-9 cells were grown between 5 and 7 days past confluence to allow for matrix accumulation. Culture medium was supplemented with 50 μg/ml ascorbic acid and replaced every 24–48 h.

7S Dodecamer Purification—PFHR-9 cells were homogenized in 1% (w/v) deoxycholate with sonication, and the insoluble material was isolated after centrifugation at 20,000 × *g* for 15 min. The pellet was then extracted with 1 M NaCl plus 50 mM Tris-Cl, pH 7.5, and 10 mM Tris-Cl, pH 7.5, and then digested in 50 mM Tris-Cl, pH 7.5, 5 mM $CaCl_2$, 5 mM benzamidine, 25 mM 6-aminocaproic acid, 0.4 mM phenylmethylsulfonyl fluoride (PMSF), and 0.1 mg/ml bacterial collagenase (Worthington). Collagenase-solubilized material was dialyzed against 50 mM Tris-Cl, pH 7.5. The 7S dodecamer was purified by anion exchange chromatography (DEAE-cellulose) followed by gel filtration chromatography. In some experiments, the 7S dodecamer was purified from matrix produced by cells grown in culture medium supplemented with inhibitors of transglutaminase (putrescine and cadaverine), peroxidasin (phloroglucinol), and lysyl oxidase (BAPN) and/or copper chelators (BCS and SCZ).

SDS-PAGE and Immunoblotting—The protein concentration was determined by a Pierce™ BCA protein assay kit using BSA as a standard protein. For immunoblotting assays, protein samples were loaded for 4–20 or 12% (w/v) SDS-PAGE and electrotransferred onto nitrocellulose membranes. Blots were incubated with polyclonal anti-7S collagen IV (Assay Biotech) or LOXL2 (Abcam) antibodies and visualized with horseradish peroxidase (HRP)-conjugated donkey anti-rabbit as secondary antibody (Jackson ImmunoResearch Laboratories). Detection of HRP activity from secondary antibodies was revealed using Pierce enhanced chemiluminescence (ECL) reagents (Thermo Scientific) following the instructions of the manufacturer. ImageJ software was used for quantification of experiments.

LOX Activity Assay—LOX enzymatic activity was measured in concentrated serum-free conditioned cell culture medium using 1,5-diaminopentane as substrate, monitoring hydrogen peroxide production by an Amplex Red fluorescence assay (Invitrogen) (56). Briefly, the enzymatic reaction was performed in 0.05 M sodium borate, pH 8.2, buffer containing 1 unit/ml horseradish peroxidase, 10 mM Amplex Red, and 10 mM 1,5-diaminopentane in the presence or absence of 1 mM BAPN. After a 30-min incubation at 37 °C, fluorescence was measured on a SpectraMax M5 plate reader using excitation and emission wavelengths of 540 and 590 nm, respectively. LOX enzymatic activity is reported as the difference in relative fluorescence units between preparations with and without BAPN.

Cloning, Plasmid Constructions, and Transient Transfection—The TrueORF Gold cDNA for human LOXL2 (C-terminal Myc-DDK-tagged) cloned in to the pCMV6 vector was purchased from Origene (Rockville, MD). A catalytically inactive mutant ($LOXL2^{Y689F}$) was generated by site-directed mutagenesis PCR (42). The following primers were designed to introduce the point mutation Y689F into the construct pCMV6-LOXL2-DDK-Myc: rhLOXL2-Y689F forward (5′-GCTGCTGGGACATGTTCCGCCATGACATCGACTG-3′) and rhLOXL2-Y689F reverse (5′-CAGTCGATGTCATGGCGGTACATGTCCCAGCAGC-3′). Clones containing $LOXL2^{Y689F}$ mutant were verified by DNA sequencing.

LOXL2 and its catalytically inactive $LOXL2^{Y689F}$ mutant were transiently transfected in HEK293 cells using Lipofectamine 2000 reagent (Invitrogen). Cells were grown for 2 days in complete medium. On the 3rd day, the culture medium was replaced with fresh serum-free DMEM/F-12 medium (without phenol red) and cultured for an extra day before evaluation of LOXL2 enzymes expression by both Western blotting and LOX activity assay.

A C-terminal His_6-tagged version of human LOXL2 was generated from LOXL2-Myc-DDK by standard cloning techniques. The resulting LOXL2-His_6-pCMV6 construct was stably transfected into HEK293 cells, and expression of LOXL2-His_6 by Geneticin-resistant clones was determined by immunoblotting using anti-LOXL2 antibody (Abcam). Stably transfected cells were expanded, and secreted LOXL2-His_6 was purified with a nickel-nitrilotriacetic acid column to >95% as

judged by SDS-PAGE. The enzymatic activity (and its inhibition by BAPN) of the purified recombinant enzyme was characterized by a LOX activity assay with diaminopentane as substrate.

Immunohistochemistry—Kidney samples from wild type C57BLKS/J (BKS) mice were prepared for immunohistochemical staining as described previously (57, 58). Briefly, under deep anesthesia with Nembutal (70 mg/kg i.p.; Abbot Laboratories), mice were exsanguinated with ~10 ml of heparinized saline (0.9% NaCl and 2 units/ml heparin) through a transcardial aortic cannula. Kidneys were perfused with fixative containing 3.7% formaldehyde, 0.01 M sodium *m*-periodate, 0.04 M sodium phosphate, 1% acetic acid, and 0.1 M NaCl. The fixed kidneys were dehydrated through a graded series of ethanols, embedded in paraffin, sectioned at 4-μm thickness, and mounted on glass slides. Kidney sections were deparaffinized and rehydrated with a battery of xylene and ethanol. Antigen retrieval was done using antigen retrieval buffer (Dako). Unspecific sites were blocked with hydrogen peroxide, biotin, avidin, and 5% normal serum blocking buffer (Abcam). Immunohistochemical staining was carried out with anti-LOXL2 antibody at 1:200. Immunoperoxidase staining was performed with an HRP/3,3′-diaminobenzidine detection kit (Abcam) following the manufacturer's instructions. Counterstaining was performed with Harris's hematoxylin (Ricca Chemical Co.). Labeled sections were imaged on a Leica microscope equipped with a Nikon DXM 1200 digital camera.

Isolation of Mouse Glomeruli—Mouse glomeruli were isolated following the procedure described by Takemoto *et al.* (59). C57BLKS/J (BKS) adult mice were perfused through the heart with magnetic 4.5-μm-diameter Dynabeads (Invitrogen) diluted in PBS. Kidneys were minced into small pieces and digested with 1 mg/ml collagenase A and 100 units/ml deoxyribonuclease in HBSS at 37 °C for 30 min. Collagenase-digested tissue was filtered two times through a 100-μm cell strainer and washed with 5 ml of HBSS each time. The cell suspension was then centrifuged at 200 × *g* for 5 min. The supernatant was discarded, and the cell pellet was resuspended in 2 ml of HBSS. Finally, glomeruli containing Dynabeads were captured with a magnetic particle concentrator and washed three times with HBSS. The purity of the glomerular preparations was >97% as assessed by inspection under a microscope. Glomeruli were used for both RNA and protein extractions.

RNA Isolation and Quantitative Real Time PCR—Total RNA was prepared using the RNeasy Mini kit (Qiagen) following the manufacturer's instructions. RNA was analyzed on 1% agarose gels to verify the RNA integrity by visualizing the 18S and 28S rRNA. RNA was quantified in a NanoDrop 2000 spectrophotometer (Thermo Scientific). One microgram of RNA was reversed transcribed into cDNA using the Script cDNA synthesis kit (Bio-Rad). Real time PCR was performed using a Bio-Rad CFX96 system in the presence of SsoAdvanced Universal SYBR Green Supermix (Bio-Rad).

Primers used for qPCR were as follows: LOX-forward, 5′-ATGTTATGACACCTATGC-3′; LOX-reverse, 5′-TACACTGACCTTTAGAATG-3′; LOXL1-forward, 5′-TCTGACTTCACCAACAAC-3′; LOXL1-reverse, 5′-ATCAGGACTGGACGATTT-3′; LOXL2-forward, 5′-TGGTTGGACAATATCTAC-3′; LOXL2-reverse, 5′-TTTAGGCTCTCTATTTGG-3′; LOXL3-forward, 5′-ACAGTATGGACATCTTCAC-3′; LOXL3-reverse, 5′-GAGACATCCTCTTGACAC-3′; LOXL4-forward, 5′-TATCTTCCAGGTGGTTGT-3′; LOXL4-reverse, 5′-CGCTGTCCATCATACTTG-3′; GAPDH-forward, 5′-GAGAAACCTGCCAAGTATG-3′; GAPDH-reverse, 5′-GGAGTTGCTGTTGAAGTC-3′. Optimization of the qPCR was performed according to the manufacturer's instructions. -Fold change in the target gene was normalized to GAPDH and calculated by the $2^{-\Delta\Delta Ct}$ method (60).

In Vitro 7S Cross-linking Experiments—For this experiment, the 7S dodecamer was purified from PFHR-9 cells grown in culture medium containing LOX inhibitor BAPN and copper chelator BCS at a concentrations of 1 mM and 100 μM, respectively (40, 51). After 7 days, 7S dodecamer (7S-BAPN/BCS) lacking LOX-mediated cross-links was purified by anion exchange and gel filtration chromatography as described above. *In vitro* cross-linking was performed by mixing recombinant LOXL2-His_6 with 7S-BAPN/BCS (molar ratio of 1:25) in 20 mM sodium phosphate buffer, pH 8. The cross-linking reaction was allowed to proceed over 92 h at 37 °C before the products were fractionated by SDS-PAGE. The signal intensity of 7S oligomers (dimers, trimmers, tetramers, pentamers, and hexamers) relative to 7S monomeric subunits was quantified with NIH ImageJ software (61).

Overlay Assays—HEK293 cells were seeded on PFHR-9 matrix prepared from cells grown in the presence of 1 mM BAPN. Once attached, HEK293 cells were transiently transfected with human LOXL2 or $LOXL2^{Y689F}$ constructs. After 48 h, culture medium was harvested for later detection of lysyl oxidase expression by immunoblotting and enzymatic activity as described above. HEK293 cells were then removed with deoxycholate, and the remaining insoluble material was digested with bacterial collagenase. 7S and NC1 domain subunits were fractionated by SDS-PAGE and analyzed by immunoblotting with collagen IV 7S and NC1 domain-specific antibodies.

Detection of Lysyl-Aldehyde Cross-links by Oxyblot Assays—Purified proteins including 7S dodecamer, 7S dodecamer isolated from cells grown with BAPN (7S-BAPN) and NC1 hexamer were deglycosylated with peptide-*N*-glycosidase F (New England BioLabs) to avoid any nonspecific derivatization of oxidized carbohydrates. Additional samples were prepared by incubating 7S-BAPN and NC1 hexamer with recombinant human LOXL2 to allow for the formation of new lysyl-aldehyde cross-links. All protein samples were denatured and reduced in a solution containing 6% SDS and 50 mM DTT. Denatured proteins were mixed with either DNPH solution or the derivatization control solution included in the Oxyblot kit (Millipore). After 10 min at room temperature, the reactions were stopped with neutralization solution. 2,4-Dinitrophenyl-derivatized proteins were fractionated in two identical SDS-polyacrylamide gels; one was stained for proteins with Coomassie Blue, and the other was electroblotted to nitrocellulose membrane for detection of carbonyl groups with anti-2,4-dinitrophenyl antibody and visualized by ECL.

Mass Spectrometry Analysis of PFHR-9 and Glomerular ECM—PFHR-9 matrix was extracted for 15 min in 50 mM Tris-Cl, pH 7.5, buffer containing 4 M guanidine HCl and 25 mM DTT. Complete dissolution of matrix proteins was achieved by placing the extract in boiling water for 5 min. Alkylation of free sulfhydryl groups was performed by adding 50 mM iodoacetamide (final concentration) to the protein solution and allowing the reaction to proceed for 30 min at room temperature in the dark. Proteins were precipitated by adding nine parts of cold ethanol and incubated for at least 1 h at −20 °C. The protein pellet was washed in cold ethanol once before resuspending proteins in 0.1 M ammonium bicarbonate, pH 7.8. The protein solution was digested with trypsin (1:20) overnight at room temperature. Tryptic peptides were dried by evaporation and submitted to the Vanderbilt Proteomics core for LC-MS/MS analyses.

Glomerular ECM (GECM) proteins were obtained from Dynabead-isolated adult mouse glomeruli using a modified version of the method of Carlson *et al.* (62). Briefly, glomeruli were suspended in 3.4 M NaCl containing 1 mM PMSF for 30 min on ice. The insoluble pellet was extracted with a 1% deoxycholate solution containing 1 mM PMSF for 1 h at room temperature. To reduce viscosity, the remaining pellet was resuspended in 1 M NaCl containing 2000 units of DNase. The pellet was extensively rinsed with water and completely dissolved after incubating in 0.01 N NaOH. The GECM protein solution was diluted with an equal volume of 0.4 M Tris-HCl buffer, pH 8.0, containing 8 M guanidine HCl and 50 mM DTT. Reduced GECM proteins were alkylated with 50 mM iodoacetamide and subjected to ethanol precipitation. GECM proteins were resuspended in 0.1 M ammonium bicarbonate and digested to peptides with trypsin (1:25) overnight at room temperature. Tryptic peptides were submitted to the Vanderbilt Proteomics laboratory for MudPIT (50). Briefly, GECM peptides were separated by a combined strong cation exchange and reversed phase chromatographic strategy. Subsets of peptides were eluted from the strong cation exchange onto the reversed phase using a series of ammonium acetate pulses of increasing concentration. This was performed for eight steps, each followed by a 105-min aqueous to organic separation on the reversed phase column. Eluted peptides were directly nanoelectrospray-ionized and introduced into an LTQ-XL mass spectrometer (Thermo Fisher Scientific) where peptide tandem mass (MS/MS) spectra were collected in a data-dependent manner.

The SEQUEST database search algorithm was used to interpret the MS/MS spectra obtained from the LC-MS/MS and MudPIT experiments. All spectra were matched to the UniProt mouse protein database plus a set of well known contaminants. Precursor and fragment ion tolerances were set at 0.5 Da. Cysteine carbamidomethylation (+57.012) was set as a static modification, and oxidation of methionine (15.9949) was considered as a variable modification. Only tryptic peptides were considered with a maximum of one missed cleavage. The searched output files for each .RAW file from MudPIT analyses were further implemented in Scaffold (version 3.3.1) for statistical analyses and protein grouping. Protein identifications were considered with a global protein false discovery rate at 1% with a minimum of two unique peptides for each protein group. Scaffold was used to compare and validate SEQUEST data. Proteins with two or more peptide identifications based on the combination of results from both database search algorithms were taken as true identifications. For the Scaffold analysis, the following probability values were selected: 95% for peptide identification calculated using Peptide Prophet software and 99% for protein identification with the additional requirement that a protein should contain at least two peptides per protein. Protein probability was calculated using the Protein Prophet algorithm within Scaffold.

Author Contributions—R. M. V. conceived and coordinated the study. C. A., A. J. L.-J., M. R., L. V. M., M.-Z. Z., and R. M. V. designed experiments and acquired and analyzed data. R. M. V. and B. G. H. interpreted data. R. M. V., C. A., and A. J. L.-J. wrote the paper. All authors reviewed the results and approved the final version of the manuscript.

Acknowledgments—We are grateful to Parvin Todd and Suwan Wang for excellent technical assistance. We also thank Kristie Rose and Hayes McDonald from the Proteomics Laboratory-Mass Spectrometry Research Center at Vanderbilt University for assistance with the Orbitrap-LTQ instrument.

References

1. Hudson, B. G., Reeders, S. T., and Tryggvason, K. (1993) Type IV collagen: structure, gene organization, and role in human diseases. Molecular basis of Goodpasture and Alport syndromes and diffuse leiomyomatosis. *J. Biol. Chem.* **268,** 26033–26036
2. Miner, J. H. (2012) The glomerular basement membrane. *Exp. Cell Res.* **318,** 973–978
3. Khoshnoodi, J., Pedchenko, V., and Hudson, B. G. (2008) Mammalian collagen IV. *Microsc. Res. Tech.* **71,** 357–370
4. Boutaud, A., Borza, D.-B., Bondar, O., Gunwar, S., Netzer, K.-O., Singh, N., Ninomiya, Y., Sado, Y., Noelken, M. E., and Hudson, B. G. (2000) Type IV collagen of the glomerular basement membrane. Evidence that the chain specificity of network assembly is encoded by the noncollagenous NC1 domains. *J. Biol. Chem.* **275,** 30716–30724
5. Timpl, R., Wiedemann, H., van Delden, V., Furthmayr, H., and Kühn, K. (1981) A network model for the organization of type IV collagen molecules in basement membranes. *Eur. J. Biochem.* **120,** 203–211
6. Yurchenco, P. D., and Furthmayr, H. (1984) Self-assembly of basement membrane collagen. *Biochemistry* **23,** 1839–1850
7. Cummings, C. F., Pedchenko, V., Brown, K. L., Colon, S., Rafi, M., Jones-Paris, C., Pokydeshava, E., Liu, M., Pastor-Pareja, J. C., Stothers, C., Ero-Tolliver, I. A., McCall, A. S., Vanacore, R., Bhave, G., Santoro, S., *et al.* (2016) Extracellular chloride signals collagen IV network assembly during basement membrane formation. *J. Cell Biol.* **213,** 479–494
8. Vanacore, R. M., Shanmugasundararaj, S., Friedman, D. B., Bondar, O., Hudson, B. G., and Sundaramoorthy, M. (2004) The α1.α2 network of collagen IV. Reinforced stabilization of the noncollagenous domain-1 by noncovalent forces and the absence of Met-Lys cross-links. *J. Biol. Chem.* **279,** 44723–44730
9. McCall, A. S., Cummings, C. F., Bhave, G., Vanacore, R., Page-McCaw, A., and Hudson, B. G. (2014) Bromine is an essential trace element for assembly of collagen IV scaffolds in tissue development and architecture. *Cell* **157,** 1380–1392
10. Fidler, A. L., Vanacore, R. M., Chetyrkin, S. V., Pedchenko, V. K., Bhave, G., Yin, V. P., Stothers, C. L., Rose, K. L., McDonald, W. H., Clark, T. A., Borza, D.-B., Steele, R. E., Ivy, M. T., Aspirnauts, T., Hudson, J. K., *et al.* (2014) A unique covalent bond in basement membrane is a primordial innovation for tissue evolution. *Proc. Natl. Acad. Sci. U.S.A.* **111,** 331–336
11. Bhave, G., Cummings, C. F., Vanacore, R. M., Kumagai-Cresse, C., Ero-Tolliver, I. A., Rafi, M., Kang, J. S., Pedchenko, V., Fessler, L. I., Fessler, J. H.,

and Hudson, B. G. (2012) Peroxidasin forms sulfilimine chemical bonds using hypohalous acids in tissue genesis. *Nat. Chem. Biol.* **8,** 784–790
12. Vanacore, R., Ham, A. J., Voehler, M., Sanders, C. R., Conrads, T. P., Veenstra, T. D., Sharpless, K. B., Dawson, P. E., and Hudson, B. G. (2009) A sulfilimine bond identified in collagen IV. *Science* **325,** 1230–1234
13. Vanacore, R. M., Friedman, D. B., Ham, A. J., Sundaramoorthy, M., and Hudson, B. G. (2005) Identification of *S*-hydroxylysyl-methionine as the covalent cross-link of the noncollagenous (NC1) hexamer of the $\alpha1\alpha1\alpha2$ collagen IV network: a role for the post-translational modification of lysine 211 to hydroxylysine 211 in hexamer assembly. *J. Biol. Chem.* **280,** 29300–29310
14. Robertson, W. E., Rose, K. L., Hudson, B. G., and Vanacore, R. M. (2014) Supramolecular organization of the α121-α565 collagen IV network. *J. Biol. Chem.* **289,** 25601–25610
15. Risteli, J., Bächinger, H. P., Engel, J., Furthmayr, H., and Timpl, R. (1980) 7-S collagen: characterization of an unusual basement membrane structure. *Eur. J. Biochem.* **108,** 239–250
16. Langeveld, J. P., Noelken, M. E., Hård, K., Todd, P., Vliegenthart, J. F., Rouse, J., and Hudson, B. G. (1991) Bovine glomerular basement membrane. Location and structure of the asparagine-linked oligosaccharide units and their potential role in the assembly of the 7 S collagen IV tetramer. *J. Biol. Chem.* **266,** 2622–2631
17. Yurchenco, P. D. (2011) Basement membranes: cell scaffoldings and signaling platforms. *Cold Spring Harb. Perspect. Biol.* **3,** a004911
18. Timpl, R., Risteli, J., and Bächinger, H. P. (1979) Identification of a new basement membrane collagen by the aid of a large fragment resistant to bacterial collagenase. *FEBS Lett.* **101,** 265–268
19. Duncan, K. G., Fessler, L. I., Bächinger, H. P., and Fessler, J. H. (1983) Procollagen IV. Association to tetramers. *J. Biol. Chem.* **258,** 5869–5877
20. Bailey, A. J., Sims, T. J., and Light, N. (1984) Cross-linking in type IV collagen. *Biochem. J.* **218,** 713–723
21. Glanville, R. W., Qian, R. Q., Siebold, B., Risteli, J., and Kühn, K. (1985) Amino acid sequence of the N-terminal aggregation and cross-linking region (7S domain) of the α1(IV) chain of human basement membrane collagen. *Eur. J. Biochem.* **152,** 213–219
22. Siebold, B., Qian, R. A., Glanville, R. W., Hofmann, H., Deutzmann, R., and Kühn, K. (1987) Construction of a model for the aggregation and cross-linking region (7S domain) of type IV collagen based upon an evaluation of the primary structure of the α1 and α2 chains in this region. *Eur. J. Biochem.* **168,** 569–575
23. Kleinman, H. K., McGarvey, M. L., Liotta, L. A., Robey, P. G., Tryggvason, K., and Martin, G. R. (1982) Isolation and characterization of type IV procollagen, laminin, and heparan sulfate proteoglycan from the EHS sarcoma. *Biochemistry* **21,** 6188–6193
24. Kagan, H. M., and Li, W. (2003) Lysyl oxidase: properties, specificity, and biological roles inside and outside of the cell. *J. Cell. Biochem.* **88,** 660–672
25. Eyre, D. R., Paz, M. A., and Gallop, P. M. (1984) Cross-linking in collagen and elastin. *Annu. Rev. Biochem.* **53,** 717–748
26. Kagan, H. M., and Ryvkin, F. (2011) Lysyl oxidase and lysyl oxidase-like enzymes. *The Extracellular Matrix: an Overview* (Mecham, R. P., ed) pp. 303–335, Springer, Berlin
27. Wang, S. X., Mure, M., Medzihradszky, K. F., Burlingame, A. L., Brown, D. E., Dooley, D. M., Smith, A. J., Kagan, H. M., and Klinman, J. P. (1996) A crosslinked cofactor in lysyl oxidase: redox function for amino acid side chains. *Science* **273,** 1078–1084
28. Reiser, K., McCormick, R. J., and Rucker, R. B. (1992) Enzymatic and nonenzymatic cross-linking of collagen and elastin. *FASEB J.* **6,** 2439–2449
29. Grau-Bové, X., Ruiz-Trillo, I., and Rodriguez-Pascual, F. (2015) Origin and evolution of lysyl oxidases. *Sci. Rep.* **5,** 10568
30. Polgar, N., Fogelgren, B., Shipley, J. M., and Csiszar, K. (2007) Lysyl oxidase interacts with hormone placental lactogen and synergistically promotes breast epithelial cell proliferation and migration. *J. Biol. Chem.* **282,** 3262–3272
31. Barry-Hamilton, V., Spangler, R., Marshall, D., McCauley, S., Rodriguez, H. M., Oyasu, M., Mikels, A., Vaysberg, M., Ghermazien, H., Wai, C., Garcia, C. A., Velayo, A. C., Jorgensen, B., Biermann, D., Tsai, D., *et al.* (2010) Allosteric inhibition of lysyl oxidase-like-2 impedes the development of a pathologic microenvironment. *Nat. Med.* **16,** 1009–1017
32. Di Donato, A., Ghiggeri, G. M., Di Duca, M., Jivotenko, E., Acinni, R., Campolo, J., Ginevri, F., and Gusmano, R. (1997) Lysyl oxidase expression and collagen cross-linking during chronic Adriamycin nephropathy. *Nephron* **76,** 192–200
33. Vadasz, Z., Kessler, O., Akiri, G., Gengrinovitch, S., Kagan, H. M., Baruch, Y., Izhak, O. B., and Neufeld, G. (2005) Abnormal deposition of collagen around hepatocytes in Wilson's disease is associated with hepatocyte specific expression of lysyl oxidase and lysyl oxidase like protein-2. *J. Hepatol.* **43,** 499–507
34. Fong, S. F., Dietzsch, E., Fong, K. S., Hollosi, P., Asuncion, L., He, Q., Parker, M. I., and Csiszar, K. (2007) Lysyl oxidase-like 2 expression is increased in colon and esophageal tumors and associated with less differentiated colon tumors. *Genes Chromosomes Cancer* **46,** 644–655
35. Barker, H. E., Cox, T. R., and Erler, J. T. (2012) The rationale for targeting the LOX family in cancer. *Nat. Rev. Cancer* **12,** 540–552
36. Erler, J. T., Bennewith, K. L., Nicolau, M., Dornhöfer, N., Kong, C., Le, Q. T., Chi, J. T., Jeffrey, S. S., and Giaccia, A. J. (2006) Lysyl oxidase is essential for hypoxia-induced metastasis. *Nature* **440,** 1222–1226
37. Bignon, M., Pichol-Thievend, C., Hardouin, J., Malbouyres, M., Bréchot, N., Nasciutti, L., Barret, A., Teillon, J., Guillon, E., Etienne, E., Caron, M., Joubert-Caron, R., Monnot, C., Ruggiero, F., Muller, L., *et al.* (2011) Lysyl oxidase-like protein-2 regulates sprouting angiogenesis and type IV collagen assembly in the endothelial basement membrane. *Blood* **118,** 3979–3989
38. Pöschl, E., Schlötzer-Schrehardt, U., Brachvogel, B., Saito, K., Ninomiya, Y., and Mayer, U. (2004) Collagen IV is essential for basement membrane stability but dispensable for initiation of its assembly during early development. *Development* **131,** 1619–1628
39. Trackman, P. C., and Kagan, H. M. (1979) Nonpeptidyl amine inhibitors are substrates of lysyl oxidase. *J. Biol. Chem.* **254,** 7831–7836
40. Tang, S. S., Trackman, P. C., and Kagan, H. M. (1983) Reaction of aortic lysyl oxidase with β-aminopropionitrile. *J. Biol. Chem.* **258,** 4331–4338
41. Hollosi, P., Yakushiji, J. K., Fong, K. S., Csiszar, K., and Fong, S. F. (2009) Lysyl oxidase-like 2 promotes migration in noninvasive breast cancer cells but not in normal breast epithelial cells. *Int. J. Cancer* **125,** 318–327
42. Lugassy, J., Zaffryar-Eilot, S., Soueid, S., Mordoviz, A., Smith, V., Kessler, O., and Neufeld, G. (2012) The enzymatic activity of lysyl oxidas-like-2 (LOXL2) is not required for LOXL2-induced inhibition of keratinocyte differentiation. *J. Biol. Chem.* **287,** 3541–3549
43. Eyre, D. R., Weis, M. A., and Wu, J. J. (2008) Advances in collagen cross-link analysis. *Methods* **45,** 65–74
44. Levine, R. L., Williams, J. A., Stadtman, E. R., and Shacter, E. (1994) Carbonyl assays for determination of oxidatively modified proteins. *Methods Enzymol.* **233,** 346–357
45. Molnar, J., Fong, K. S., He, Q. P., Hayashi, K., Kim, Y., Fong, S. F., Fogelgren, B., Szauter, K. M., Mink, M., and Csiszar, K. (2003) Structural and functional diversity of lysyl oxidase and the LOX-like proteins. *Biochim. Biophys. Acta* **1647,** 220–224
46. Moon, H. J., Finney, J., Xu, L., Moore, D., Welch, D. R., and Mure, M. (2013) MCF-7 cells expressing nuclear associated lysyl oxidase-like 2 (LOXL2) exhibit an epithelial-to-mesenchymal transition (EMT) phenotype and are highly invasive *in vitro*. *J. Biol. Chem.* **288,** 30000–30008
47. Vanacore, R., Pedchenko, V., Bhave, G., and Hudson, B. G. (2011) Sulphilimine cross-links in Goodpasture's disease. *Clin. Exp. Immunol.* **164,** Suppl. 1, 4–6
48. Tanzer, M. L. (1967) Collagen crosslinks: stabilization by borohyride reduction. *Biochim. Biophys. Acta* **133,** 584–587
49. Rodriguez, H. M., Vaysberg, M., Mikels, A., McCauley, S., Velayo, A. C., Garcia, C., and Smith, V. (2010) Modulation of lysyl oxidase-like 2 enzymatic activity by an allosteric antibody inhibitor. *J. Biol. Chem.* **285,** 20964–20974
50. Link, A. J., Eng, J., Schieltz, D. M., Carmack, E., Mize, G. J., Morris, D. R., Garvik, B. M., and Yates, J. R., 3rd. (1999) Direct analysis of protein complexes using mass spectrometry. *Nat. Biotechnol.* **17,** 676–682
51. Higgins, D. F., Kimura, K., Bernhardt, W. M., Shrimanker, N., Akai, Y., Hohenstein, B., Saito, Y., Johnson, R. S., Kretzler, M., Cohen, C. D., Eck-

ardt, K. U., Iwano, M., and Haase, V. H. (2007) Hypoxia promotes fibrogenesis *in vivo* via HIF-1 stimulation of epithelial-to-mesenchymal transition. *J. Clin. Investig.* **117,** 3810–3820

52. Martin, A., Salvador, F., Moreno-Bueno, G., Floristán, A., Ruiz-Herguido, C., Cuevas, E. P., Morales, S., Santos, V., Csiszar, K., Dubus, P., Haigh, J. J., Bigas, A., Portillo, F., and Cano, A. (2015) Lysyl oxidase-like 2 represses Notch1 expression in the skin to promote squamous cell carcinoma progression. *EMBO J.* **34,** 1090–1109
53. Lorz, C., Benito-Martín, A., Boucherot, A., Ucero, A. C., Rastaldi, M. P., Henger, A., Armelloni, S., Santamaría, B., Berthier, C. C., Kretzler, M., Egido, J., and Ortiz, A. (2008) The death ligand TRAIL in diabetic nephropathy. *J. Am. Soc. Nephrol.* **19,** 904–914
54. Neusser, M. A., Lindenmeyer, M. T., Moll, A. G., Segerer, S., Edenhofer, I., Sen, K., Stiehl, D. P., Kretzler, M., Gröne, H. J., Schlöndorff, D., and Cohen, C. D. (2010) Human nephrosclerosis triggers a hypoxia-related glomerulopathy. *Am. J. Pathol.* **176,** 594–607
55. Brukamp, K., Jim, B., Moeller, M. J., and Haase, V. H. (2007) Hypoxia and podocyte-specific Vhlh deletion confer risk of glomerular disease. *Am. J. Physiol. Renal Physiol.* **293,** F1397–F1407
56. Palamakumbura, A. H., and Trackman, P. C. (2002) A fluorometric assay for detection of lysyl oxidase enzyme activity in biological samples. *Anal. Biochem.* **300,** 245–251
57. Zhao, H. J., Wang, S., Cheng, H., Zhang, M. Z., Takahashi, T., Fogo, A. B., Breyer, M. D., and Harris, R. C. (2006) Endothelial nitric oxide synthase deficiency produces accelerated nephropathy in diabetic mice. *J. Am. Soc. Nephrol.* **17,** 2664–2669
58. Zhang, M. Z., Wang, S., Yang, S., Yang, H., Fan, X., Takahashi, T., and Harris, R. C. (2012) Role of blood pressure and the renin-angiotensin system in development of diabetic nephropathy (DN) in eNOS−/− db/db mice. *Am. J. Physiol. Renal Physiol.* **302,** F433–F438
59. Takemoto, M., Asker, N., Gerhardt, H., Lundkvist, A., Johansson, B. R., Saito, Y., and Betsholtz, C. (2002) A new method for large scale isolation of kidney glomeruli from mice. *Am. J. Pathol.* **161,** 799–805
60. Livak, K. J., and Schmittgen, T. D. (2001) Analysis of relative gene expression data using real-time quantitative PCR and the $2^{-\Delta\Delta CT}$ method. *Methods* **25,** 402–408
61. Schindelin, J., Arganda-Carreras, I., Frise, E., Kaynig, V., Longair, M., Pietzsch, T., Preibisch, S., Rueden, C., Saalfeld, S., Schmid, B., Tinevez, J. Y., White, D. J., Hartenstein, V., Eliceiri, K., Tomancak, P., *et al.* (2012) Fiji: an open-source platform for biological-image analysis. *Nat. Methods* **9,** 676–682
62. Carlson, E. C., Brendel, K., Hjelle, J. T., and Meezan, E. (1978) Ultrastructural and biochemical analyses of isolated basement membranes from kidney glomeruli and tubules and brain and retinal microvessels. *J. Ultrastruct. Res.* **62,** 26–53